Signals from a Moving Object of Autodyne Radars with Linear Frequency Modulation

Kirill A. Ignatkov, Vladislav Ya. Noskov, Andrey P. Chupahin
Ural Federal University
Yekaterinburg, Russia
k.a.ignatkov@gmail.com

Gennadiy P. Ermak, Alexander S. Vasiliev,
O.Ya. Usikov Institute for Radio Physics and Electronics
Kharkiv, Ukraine
ermak@ire.kharkov.ua

Sergey M. Smolskiy
National Research University "Moscow Power Engineering Institute"
Moscow, Russia
smolskiysm@mail.ru

Abstract

The results of signal peculiarities' investigation of an autodyne short-range radar system with linear frequency modulation for the moving reflecting object are described. The autodyne signal plots are obtained for the cases when its period duration is much longer than delay time of the reflected emission as well as for the cases when this inequality is not satisfied. Experimental data are obtained on the 8mm-range Gunn-diode oscillator with frequency tuning by the varicap.

1 Introduction

Autodyne short-range radars with frequency modulation (FM ASRR) have a simple structure and low cost of the transceiver device. Therefore, they are widely used as the guard sensors, the anti-collision sensors of transport facilities, measuring devices of car movement parameters on hump yards, detectors of point occupation and railway crossings and many others [1–6].

A large number of publications is devoted to the research analysis of FM ASRR signal formation features (see, for example, [7–9]). They apply different mathematical oscillator models and various representations of impact functions of the proper reflected emission for the description of autodyne behavior. In a number publications of the last years the specificity of FM ASRR signal formation is considered from the point of view of the reflected emission phase delay [10, 11]. This approach, to our mind, reflects the phenomena sense in the coupled system "oscillator-reflecting object» in the most adequate manner. In this publication, for example, the nature of the experimentally observed phenomenon of the anharmonic autodyne signal distortion is proved (see the review [12]). These features, in last years, have been extensively discussed in publications devoted to semiconductor FM laser autodynes [13–15].

However, in the known researches, the solution of equations obtained for developed models is valid only for conditions, when the delay τ of reflected emission is essentially less than autodyne signal period T_a: $\tau \ll T_a$. In actual operation conditions of FM ASRR, at the increasing of distance to the radar object, this inequality may be broken. Signal formation peculiarities under these conditions were described in reports [16, 17]. However, in these publications, the influence of the object movement displacement was ignored.

The goal of this research is to reveal the general equations and to perform on its base the investigation complex of signal generation features depending on modulation parameters and FM ASRR operation conditions, which take into consideration not only the distance to the reflecting object, but its movement velocity as well.

2 Initial Expressions for Signal Analysis

A system of linearized (in the vicinity of a steady-state) differential equations for small relative variations of the amplitude α and the frequency χ for a single-circuit oscillator being under impact of the proper reflected emission has a view [18, 19]:

$$\left(\frac{Q_L}{\omega_{cav}}\right)\left(\frac{da}{dt}\right) + \alpha a + \varepsilon\chi = \Gamma(t,\tau)\eta cos\delta(t,\tau) \quad (1)$$

$$\beta a + Q_L\chi = \Gamma(t,\tau)\eta sin\delta(t,\tau) \quad (2)$$

Where Q_L,ω_{cav} are the loaded Q-factor and the cavity frequency, relatively; α,ε, and β are dimensionless parameters defining the oscillator increment slope, non-isodromity and non-isochronity, relatively; $\Gamma(t,\tau) = \Gamma_0[A(t,\tau)/A(t)]$, $\delta(t,\tau) = \Psi(t) - \Psi(t,\tau)$ are the modulus and the phase of instantaneous reflection factor presented to the oscillator output; Γ_0 is the emission damping factor in amplitude at its propagation to the object and back; $A(t,\tau)$, $\Psi(t,\tau)$ are the oscillation amplitude and phase from the system pre-history $(t-\tau)$; $\eta = Q_L/Q_{ex}$, Q_{ex} are efficiency and the external Q-factor of the oscillating system; $A(t)$, $\Psi(t)$ are the current amplitude and phase at *t* moment; $\tau = 2l/c$, where *l* is a distance to the reflecting object, and *c* is the velocity of emission propagation.

At FM of the oscillator by the variation of the vericap bias voltage, both frequency and the "patrasitic" amplitude modulation (PAM) if emission occur:

$$\omega(t) = \omega_0 + \Delta\omega_{FM}(t) = \omega_0[1 + m_{FM}f_{mod}(t)] \quad (3)$$

$$A(t) = A_0[1 + a_{AM}(t)] = A_0[1 + m_{AM}f_{mod}(t)] \quad (4)$$

where $m_{FM} = \Delta\omega_{FM}/\omega_0$ and $m_{AM} = \Delta A_{AM}/A_0$ are coefficients of frequency (FM) and amplitude (AM) modulation, relatively; $\Delta\omega_{FM}$, ΔA_{AM} are maximal deviations of amplitude and phase from theirк steady-state values A_0 and ω_0 due to oscillation modulation; $f_{mod}(t)$ is the normalized modulating function. The quasi-periodic solution of the first approximation [20] of equation system (1), (2) with account of (3), (4) for relative variations of the amplitude $a(t,\tau)$ and the absolute variations of autodyne oscillation frequency $\omega(t,\tau)$ has a form:

$$a(t,\tau) = -m_{AM}f_{mod}(t) + \Gamma(t,\tau)K_a cos[\delta(t,\tau) - \psi] \quad (5)$$

$$\omega(t,\tau) = \omega_0\{1 - m_{FM}f_{mod}(t) - \Gamma(t,\tau)\, L_a sin[\delta(t,\tau) + \theta]\} \quad (6)$$

where K_a, L_a are coefficients of autodyne amplification and the frequency deviation, relatively; $\psi = arct(\rho)$, $\theta = arct(\gamma)$ are angles of phase shift; $\rho = \varepsilon/Q_L$, $\gamma = \beta/\alpha$ are coefficients of oscillator non-isodromity and non-isochronity, relatively.

To obtain expressions describing an autodyne response in general case of arbitrary ratio of delay time τ of reflected emission and the period T_a, we use the known approach to analysis of retarded systems, which was developed for the case of signal description of usual autodynes (without FM) in [18]. Its essence consists in expansion of functions $A(t,\tau)$ and $\Psi(t,\tau)$ of delayed impact in the Tailor series over small parameter – the delay time τ with respect to the current time t. St that, we assume an absence of functions (5), (6) breaks over all time interval of the autodyne response formation. In addition, we here exclude from consideration the transients in the oscillator in reverse the zones of modulating function. Then, taking above-mentioned into account, expressions for $\Gamma(t,\tau)$ and $\delta(t,\tau)$ in (5), (6) as functions of normalized (dimensionless) delay tine $\tau_n = \omega_0\tau/2\pi$, take a view:

$$\Gamma(t_n,\tau_n) = \Gamma_0\{1 + 2\pi r_n\}\Gamma K_a \sum_{m=0}^{M}(-1)^m X_m(r_n) sin[\delta(t_n,\tau_n) - \psi + \Theta_m(r_n)] \quad (7)$$

$$\delta(t_n,\tau_n) = 2\pi\tau_n + \pi B_{FM} f_{mod}(t) - C_{FB}\sum_{m=0}^{M}(-1)^m X_m(r_n) sin[\delta(t_n,\tau_n) + \theta + \Theta_m(r_n)] \quad (8)$$

where $r_n = \tau/T_a$ is the parameter of normalized (with respect to autodyne signal period) distance to the reflecting object; $B_{FM} = \Delta F_{FM}\tau$ is the parameter of "FM base", which defines a number of signal periods keeping within a period of the modulating function at fixed reflecting object; $\Delta F_{FM} = \Delta\omega_{FM}/2\pi$; C_{FB} is the feedback parameter of the autodyne system; $t_n = \Omega_{mod}t/2\pi$ is the normalized time of the modulating function; Ω_{mod} is the modulation frequency; $X_m(r_n)$, $\Theta_m(r_n)$ are amplitude values and phase shifts of series *m*-th terms ($m = 0,1,\dots M$) in expressions (7) and (8):

$$X_m(r_n) = \frac{(2\pi r_n)^{2m}\sqrt{4(m+1)^2+(2\pi r_n)^2}}{2(m+1)\cdot(2m+1)!}, \quad \Theta_m(r_n) = -arctg\frac{\pi r_n}{(m+1)} \quad (9)$$

Then, we take into consideration some features of FM SRR functioning. At frequency control with the help of the varicap, the PAM deep is usually small. In addition, we may neglect autodyne amplitude variations $\Gamma_0 K_a$: $\Gamma_0 K_a \ll 1$.

Therefore, in expression (7), the second term in large parenthesis may be neglected. This approximation in mathematical model of the autodyne system assumes the account of the phase delay only of the reflected emission. At that, we note that known solutions [12] for autodyne response, which follow from (7) – (9), are obtained in the first approximation supposing $m = 0$. The account of series terms of higher orders in these expressions allows, as shown below, taking into consideration also the phase variation $\delta(t_n,\tau_n)$ dynamics of reflected emission.

In this connection, expressions for normalized (with respect to maximal values) variations of amplitude and frequency in the form of autodyne amplitude (AAC) $a_n(t_n,\tau_n)$ and frequency (AFC) $\chi_n(t_n,\tau_n)$ have a view:

$$a_n(t_n,\tau_n) = \frac{a(t_n,\tau_n)}{\Gamma_0 K_a} = cos[\delta(t_n,\tau_n) - \psi] \quad (10)$$

$$\chi_n(t_n,\tau_n) = \frac{\chi(t_n,\tau_n)}{\Gamma_0 L_a} = -sin[\delta(t_n,\tau_n) + \theta] \quad (11)$$

Solution of transcendent equation (8) under condition of its smoothness, when $C_{FB} < 1$, we obtain by the method of successive approximations. This solution in the form of autodyne phase characteristic (APA) $\delta(t_n,\tau_n)$ has a view:

$$\delta(t_n,\tau_n) = \delta(t_n,\tau_n)_{(0)} - C_{FB}\sum_{m=0}^{M}(-1)^m X_m(r_n) sin\big[\delta(t_n,\tau_n)_{(1)} + \theta + \Theta_m(r_n) - C_{FB}\sum_{m=0}^{M}(-1)^m X_m(r_n) sin\big[\delta(t_n,\tau_n)_{(2)} + \theta + \Theta_m(r_n) - \dots - C_{FB}\sum_{m=0}^{M}(-1)^m X_m(r_n) sin\big[\delta(t_n,\tau_n)_{(k)} + \theta + \Theta_m(r_n)\big] \dots\big]\big] \quad (12)$$

where the approximation order is denoted by indices in parenthesis near terms $\delta(t_n,\tau_n)$; $\delta(t_n,\tau_n)_{(0,1,\dots k)} = 2\pi\tau_n + \pi B_{FM} f_{mod}(t_n)$.

Zero approximation, when we take into account in (12) the first term only $\delta(t_n,\tau_n)_0$ of the sum, corresponds to the linear phase characteristics, which is typical for the homodyne SRR. The next approximations insert nonlinearity in this function, which is the attribute of the autodyne systems caused by autodyne frequency variations. Therefore, the main attention in fulfilled research will be paid to revealing signal features of FM ASRR under conditions when the C_{FB} parameter is commensurable with the unity.

Then, taking into consideration the movement of reflecting object in autodyne characteristics (10) – (12), in the first term of the right-part of (8) and (12) $\delta(t_n,\tau_n)_{(0)}$, we use substitution: $\tau_n = \tau_{0n} + \tau_n(t_n)$. As a result, we obtain:

$$\delta(t_n)_{(0)} = 2\pi\tau_{0n} + 2\pi B_{DS}\tau_n(t_n) + \pi B_{FM} f_{mod}(t_n) + 2\pi B_{DS}\chi_{FM}\tau_n(t_n) f_{mod}(t_n) \quad (13)$$

where $\tau_{0n} = \omega_0\tau_0/2\pi$ is the initial value of normalized distance; $B_{DS} = (\Omega_D/\Omega_{mod})$ is a parameter of "Doppler signal base" showing how much periods of the Doppler signal is kept within the modulation period; Ω_D id the Doppler

frequency; $\chi_{FM} = (\Delta\omega_{FM}/\omega_0)$ is the relative value of frequency deviation under modulation; $\tau_n(t_n)$ is the alternate component of the normalized distance caused by the reflecting object movement.

Now, functions (10) – (12) with account of (13) depend on one variable t_n: $\delta(t_n, \tau_n) \equiv \delta(t_n)$, $a_n(t_n, \tau_n) \equiv a_n(t_n)$, and $\chi_n(t_n, \tau_n) \equiv \chi_n(t_n)$. At that, we may neglect the last term in (13) as $2\pi B_{DS}\chi_{FM} \ll 1$.

3 Numerical Signal Analysis at FM On Saw-Tooth Non-Symmetric Law

Signals of FM ASRR are usually registered in the power source circuit of the UHF oscillator (the auto-detection signal) or by detection of oscillation amplitude variations. Both oscillation amplitude variations in the form of AAC $a_n(t_n)$ and the current autodyne frequency variations in the form of AFC $\chi_n(t_n)$ make a contribution into these signal formation. For clarification of autodyne signal formation features from the moving object, we perform calculations and an analysis of FM ASRR signals for the non-symmetric saw-tooth law. Mathematical expression for this law takes a form:

$$f_{mod}(t_n) = (2/\pi)arctgtg[(2\pi t_n + \pi)/2] \tag{14}$$

The time diagrams of APC $\delta(t_n)$, their time-derivatives $d\delta(t_n)/dt_n$, AAC $a_n(t_n)$ (curves 1) and AFC $\chi_n(t_n)$ (curves 2) calculated according (8) – (12) with account of (13), (14) for $B_{DS} = \pm 1$ are presented in Figure 1 for the case of arriving
(a–d) and departing (e–h) object for various normalized distance r_n to the reflecting object. In the vase of arriving object, a sign at B_{DS} parameter in (13) will be negative, while at deprating one the sign will be positive. For these cases of normalized distances presented in r_n, the signal spectrograms were calculated, which are presented in Figure 2. The ac component of the normalized distance $\tau_n(t_n)$, caused by the reflecting object displacement, was included in calculation according (13) by the function:

$$\tau_n(t_n) = (1000/2\pi)\sin(2\pi t_n/1000) \tag{15}$$

Diagrams presented in Figures 1 and 2 here and later, if there is no special dtupulation, are obtained at $\theta = 1, \psi = 0.2, B_{FM} = 5, B_{DS} = 0;\ C_{FB} = 0.8, k = M = 50$. Hereinafter, we shall call the segments of normalized distance r_n, which are multiplies to integers, as corresponding to the "operation zones" starting from the first where $0 \le r_n \le 1$. We note, that numbers M of series terms in (7), (8) and approximation of k order in (12) taken in calculations provide convergence of calculation results in the range of $r_n \le 5$ and $C_{FB} \le 0.98$.

From comparison of temporal and spectral diagrams (see Figures 1 and 2) we see that the sign changing of the radial velocity causes the signal frequency variation only by the Doppler shift value. For the arriving object, the signal frequency in this case decreases while for departing it increases.

From the analysis of temporal and spectral diagrams in Figures 1,a,e and 2,, we see that results obtained for the case $r_n = 0$ correspond to research results of FM ASRR signal investigation, which were resulted in publications [10, 12]. In these publications, the autodyne response formation features were considered in first approximation only, when inequality $\tau \ll T_a$ is satisfied. At that, it was shown that the phase incursion $\delta(t_n)$ irregularity of the reflected wave is caused by frequency variations $\chi_n(t_n)$.

Anharmonic distortions of the signal characteristics manifesting in "wave slope" variations depend on the C_{FB} parameter value, the character (increase or decrease) of modulating function, and on the oscillator internal parameters. The speed of phase incursion changing $d\delta(t_n)/dt_n$, characterizing as the instantaneous frequency difference of radiate and reflected oscillations, has, at that, the oscillating character with the peak formation of instantaneous frequency (see Figures 1,a,e). The peak height increases with the growth of C_{FB} parameter, which, in turn, depends also on the oscillator internal parameters and on the level of the reflected emission level. It is proved that average values of the instantaneous frequency during modulation period are equal to signal frequency in homodyne FM ASRR under condition of inequality $C_{FB} < 1$ fulfillment.

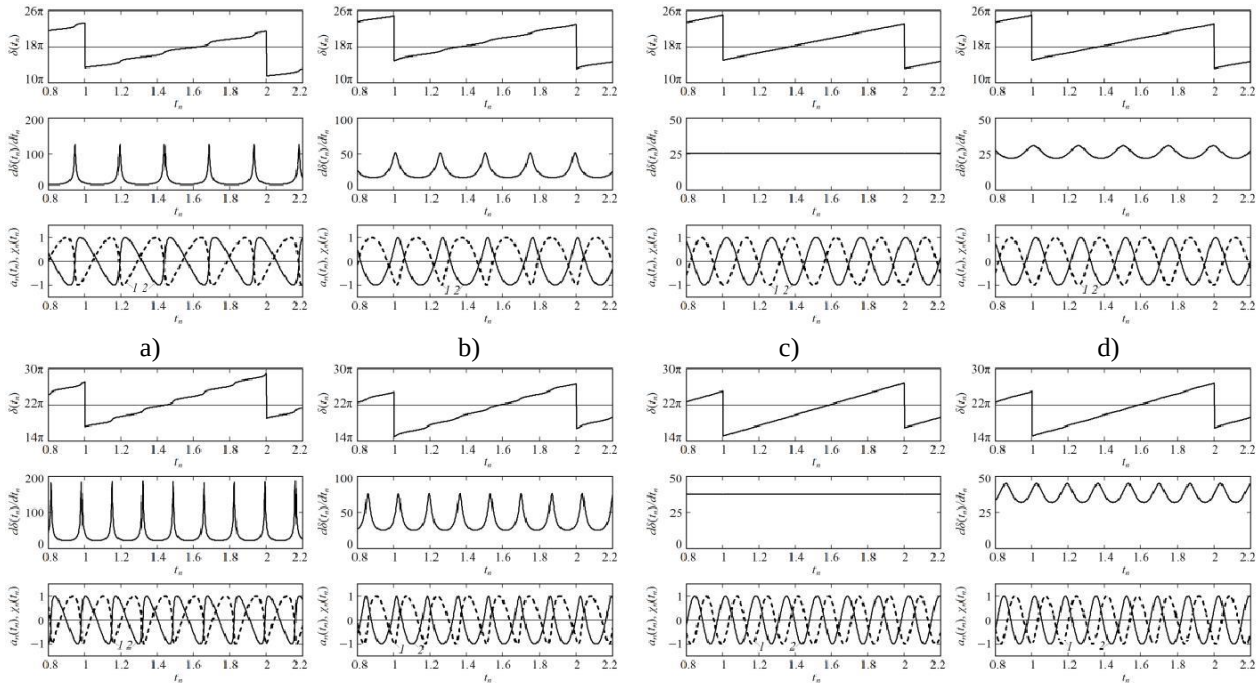

Figure 1: Time diagrams of APC $\delta(t_n)$, their derivatives $d\delta(t_n)/dt_n$, AAC $a_n(t_n)$ formation (curves 1) and AFC $\chi_n(t_n)$ (curves 2), calculated for the cases of arriving (a–d) and departing (e–h) reflecting object and for various values of normalized distance rr_n: $r_n = 0\ (a), r_n = 0.5\ (b), r_n = 1\ (c), r_n = 1.5\ (d)$

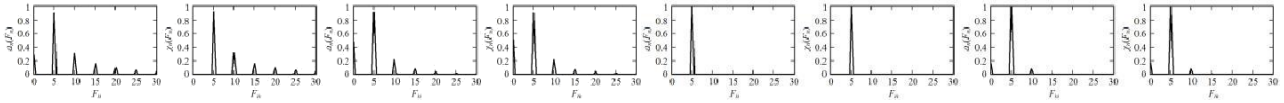

Figure 2: Spectrograms $a_n(F_n)$ and $\chi_n(F_n)$ calculated for increasing and decreasing modulating function and normalized distances $r_n = 0\ (a), r_n = 0.5\ (b), r_n = 1\ (c), r_n = 1.5\ (d)$

In the considered case (arbitrary ratio of τ and T_a), with the growth of normalized distance r_n, as it is seen from curves in Figures 1,b–d and 1,f–h, the shape of the temporal APC $\delta(t_n)$ approaches to the linear function. At that, the peak height of normalized derivative $d\delta(t_n)/dt_n$, the degree of anharmonic distortions of AAC and AFC diagrams essentially decreases. Especially, this tendency is clear in the first operation zone where $0 \le r_n \le 1$. Calculations of characteristics for other values of normalized distance r_n show that in the case of r_n values, which are multiplies to the integer number ($r_n = 1,2, \dots$), AFC and AAC have practically sine view.

From the spectrograms presented in Figure 2,c,d we can see that in the case considered, with the growth of normalized distance r_n the higher harmonics level sharply decreases. The harmonic coefficient THD is the generalized parameter, which characterizes the distortion degree of quasi-periodic oscillations. Calculation results of these coefficients are presented in Figure 3 in the form of $THD(r_n)$ for different values of C_{FB}. We took into account in these plots calculation the amplitudes of the first ten harmonic components of the Fourier series expansion.

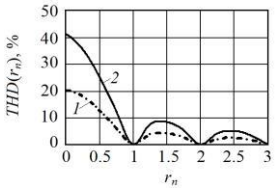

Figure 3: Plots of total harmonic distortion coefficient $THD(r_n)$ versus normalized distance r_n calculated for $B_{FM} = 5$ and $C_{FB} = 0.4$ (curve 1) and $C_{FB} = 0.8$ (curve 2)

From the plots in Figure 3 obtained, one can see that the largest distortions of FM ASRR signals are observed in the region of small values of the first operation zone. For $C_{FB} = 0.8$, the harmonic coefficient in this zone achieves approximately 40%. With further transition to higher-order operation zones, as we mentioned above, signal distortions significantly decrease achieving minimal values when normalized distance r_n is a multiple of the integer ($r_n = 1,2, \ldots$).

Returning to analysis of calculation results presented in Figure 2, it is necessary to note the presence of DC components $a_0(F_n)$ and $\chi_0(F_n)$ in spectrograms in Figures 2,c,b,d. The presence of DC component $\chi_0(F_n)$ in the oscillator response on frequency variation $\chi_n(t_n)$ in definite operation zones indicate some offset of frequency average value under the impact of reflected signal. These components deserve special attention while studying FM ASRR signals. Their account may be necessary, for instance, at signal processing, during the analysis of system noise immunity etc.

Calculation results of relative levels of DC components $a_0(r_n)$ and $\chi_0(r_n)$ depending on the normalized distance r_n values at $C_{FB} = 0.8$ are presented in Figure 4 for autodyne responses $a_n(t_n)$ and $\chi_n(t_n)$.

From obtained curves in Figure 4, one can see that in the first operation zone of FM SRR for large values of parameter C_{FB}, when the $C_{FB} \sim 1$, the DC level may have values, which are commensurable with amplitudes of the signal. Inside the higher-order zones, we can neglect by the DC component influence. We should also note that when the inequality $C_{FB} \ll 1$ is true, DC components in the FM ASRR output signals are practically eliminated.

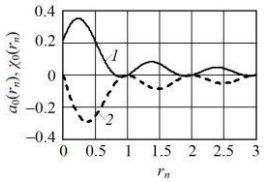

Figure 4: Plots of DC components $a_0(r_n)$ (curve 1) and $\chi_0(r_n)$ (curve 2) versus normalized distance r_n, calculated at $B_{FM} = 5$ and $C_{FB} = 0.8$.

4 Numerical Signal Analysis at FM with Saw-Tooth Symmetric Law

Now we consider the case of FM ASRR with the saw-tooth symmetric law. This law has two parts with constant derivative in each period of the modulating function but with different signs. Mathematical expression of this law has a view:

$$f_{mod}(t_n) = \left(\frac{2}{\pi}\right) \arcsin sin\,(2\pi t_n) \tag{16}$$

The time diagrams of formation of APC $\delta(t_n)$, its derivative $d\delta(t_n)/dt_n$, AAC $a_n(t_n)$ (curves 1) and AFC $\chi_n(t_n)$ (curves 2) are presented in Figure 5 for the case of arriving (a–d) and departing (e–h) object, calculated according to (8) – (12) and (13), (16) at $B_{DS} = \pm 1$ for different normalized distance r_n to the reflecting object. The signal spectrograms presented in Figure 6 were calculated for the same cases and normalized distances r_n.

From comparison of temporal and spectral diagrams of Figures 5 and 6 it follows that when changing the radial velocity sign the average value of signal frequency over modulation period does not change. In the case of arriving

object, the autodyne response frequency, on the ascending part of modulation characteristic, decreases by the Doppler shift value while on the descending part – it increases by the same value. Motion direction change leads to changing of described order to the reverse one.

At that, we should note that the growth of signal frequency in one half-period and frequency reduction in the other half-period in the case of the moving reflector and change of this order at changing of the motion direction (see Figure 5) are in full correspondence with homodyne radar systems theory [9]. This phenomenon is widely used at SRR signal processing and for range information extraction, the object velocity and its motion direction.

Difference with the FM ASRR consists in presence of its anharmonic distortions under condition, when $C_{FB}\sim 1$, and arrival of the additional phase shift caused by dynamics of autodyne variations of oscillation frequency. At that, signal spectrum "sprawling" (see Figure 6,a–d) takes place similar to the spectrum of frequency-shift keyed oscillation [21]. Here, higher harmonics and components of their combinative interaction are present as well as low-frequency components on modulation frequency corresponding to the frequency shift from the moving reflecting object and DC component.

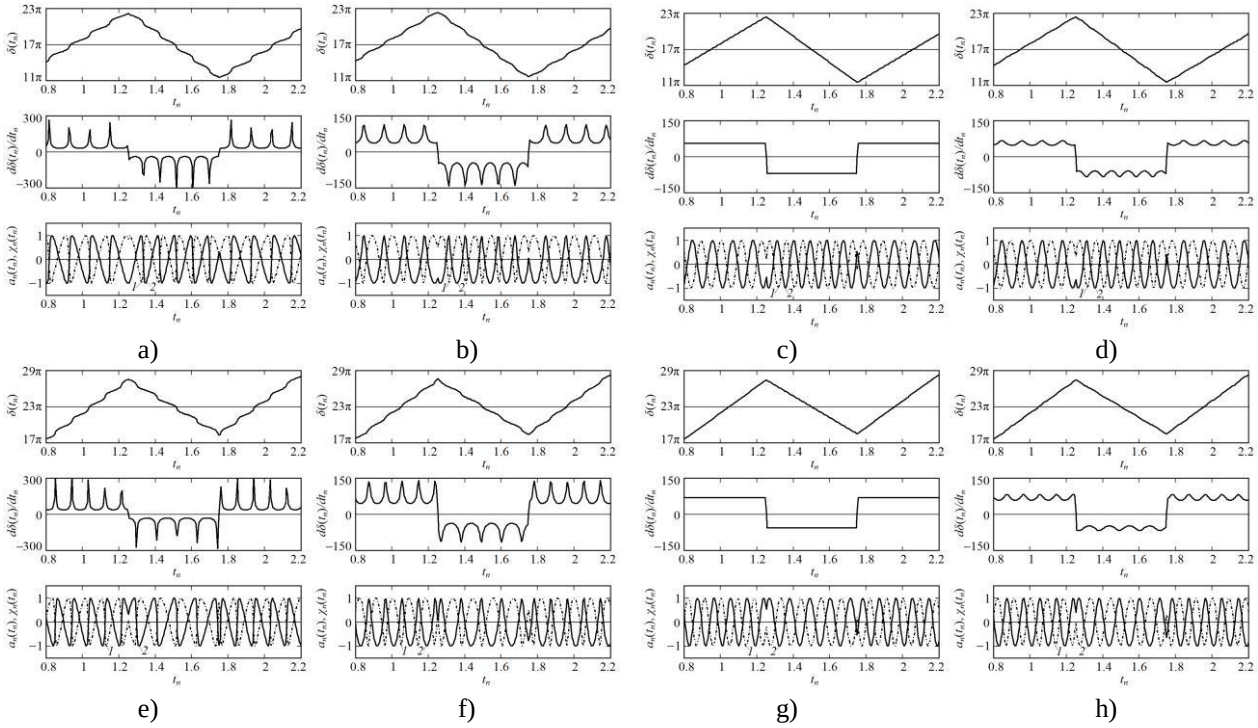

Figure 5: Time diagrams of formation of APC $\delta(t_n)$ their derivatives $d\delta(t_n)/dt_n$, AAC $a_n(t_n)$ (curves 1) and AFC $\chi_n(t_n)$ (curves 2), calculated for cases of the arriving (a–d) and departing (e–h) reflecting object at different normalized distances: $r_n = 0\ (a), r_n = 0.5\ (b), r_n = 1\ (c)$ and $r_n = 1.5\ (d)$

From spectrograms presented in Figure 6,b–d, we see that in the case under consideration, the level of higher harmonic components essentially decreases at growth of the normalized distance r_n. THD calculation results versus normalized distance r_n are presented in Figure 7 in the form of $THD(r_n)$ for various values of C_{FB}.

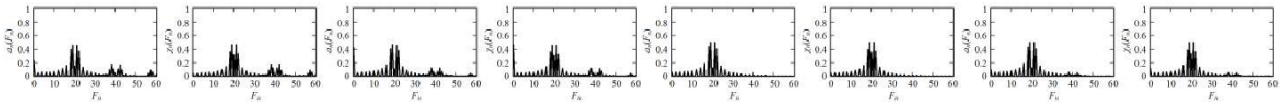

a) b) c) d)

Figure 6: Spectrograms $a_n(F_n)$ and $\chi_n(F_n)$, calculated for the case of the moving reflecting object during modulation period for different normalized distances r_n to the reflecting object: $r_n = 0\ (a), r_n = 0.5\ (b), r_n = 1\ (c)$ and $r_n = 1.5\ (d)$

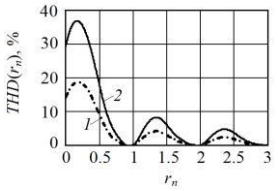

Figure 7: Plots $THD(r_n)$ versus normalized distance r_n, calculated for $B_{FM} = 5$ and $C_{FB} = 0.4$ (curve 1) and $C_{FB} = 0.8$ (curve 2)

From the obtained plots in Figure 7, one can see that the largest FM ASRR signal distortions for symmetrical law are observed in the middle part of the first operation zone. For $C_{FB} = 0.8$, the harmonic coefficient achieves here the value of 40%. With further transition to operation zones of higher order, as it was mentioned above, signal distortions essentially decrease.

Returning to spectrograms in Figure 6, it is necessary to note also the DC presence of $a_0(F_n)$ and $\chi_0(F_n)$. Calculation results of relative levels of DC components $a_0(r_n)$ and $\chi_0(r_n)$ depending on normalized distance value r_n at $C_{FB} = 0.8$ for autodyne responses $a_n(F_n)$ and $\chi_n(F_n)$ are presented in Figure 8. From comparison of obtained curves in Figures 4 and 8, it is seen that they practically coincide.

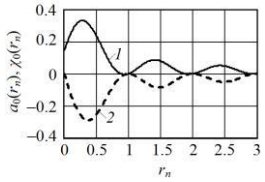

Figure 8: Plots of DC component levels $a_0(r_n)$ (curve 1) and $\chi_0(r_n)$ (curve 2) versus normalized distance r_n, calculated for $B_{FM} = 5$ and $C_{FB} = 0.8$

Thus, peculiarities of FM ASRR signal formation for symmetric saw-tooth law are described in the general case of arbitrary ration of the delay time τ of the reflected emission and the signal period T_a .

5 General Property of Signal Characteristic at FM with the Saw-Tooth Law

To explain the character of obtained functions of normalized distance r_n we introduce concepts of the equivalent feedback parameter $\mathrm{C_{eq}}$ of the autodyne system "FM ASRR – the reflecting object" and an angle of dynamic displacement of the phase $\Delta\delta_{\mathrm{DD}}$ of the autodyne response: $\mathrm{C_{eq}} = \mathrm{C_{FB}K_{DF}}$ and $\Delta\delta_{\mathrm{DD}} = \delta(\mathrm{r_n}) - \delta(\mathrm{r_n} = 0)$. Here $\mathrm{K_{DF}} = \sum_{\mathrm{m}=0}^{\mathrm{M}}(-1)^{\mathrm{m}}\mathrm{X_m(r_n)}$ is the "dynamic factor" of feedback included into (8) and (12); $\delta(\mathrm{r_n}), \delta(\mathrm{r_n} = 0)$ are phases of an instantaneous reflection factor obtained for the current value of normalized distance $\mathrm{r_n}$ and its zero value, relatively. Calculation results of functions $\mathrm{K_{DF}(r_n)}$ and $\Delta\delta_{\mathrm{DD}}(\mathrm{r_n})$ are presented in Figure 9, at that, for the function $\Delta\delta_{\mathrm{DD}}(\mathrm{r_n})$, two curves are determined: for non-isochronous (curve 1) and isochronous (curve 2) oscillators.

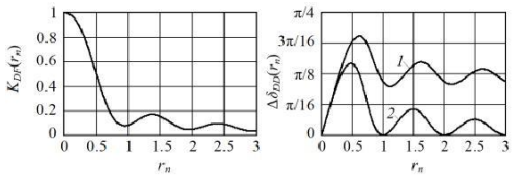

a) b)

Figure 9: Plots of the dynamic factor function $K_{DF}(r_n)$ (a) of feedback of FM ASRR and phase shift $\Delta\delta_{DD}(r_n)$ (b) signals versus normalized distance (r_n) to the reflecting object: $\theta = 1$ (curve 1), $\theta = 0$ (curve 2)

From the curve $K_{DF}(r_n)$ (see Figure 9,a) one can see that with growth of normalized distance r_n in the first operation zone where $0 < r_n < 1$, the K_{DF} value and relatively the value of equivalent parameter C_{eq} decreases almost by the order. Further, with growth of r_n, the value of C_{eq} asymptotically damps with slight increase in the middle parts of higher operation zones where $r_n > 1$.

Dynamic phase variations $\Delta\delta_{DD}$ of signal characteristics influencing on character of their distortions, which is well seen from comparison of curves in Figures 1,a,b; 1,e,f; 5,a,b, and 5,e,f, are also small at r_n increase in the first zone. At $r_n = 1$, there is the first minimum of this value, which is determined by the θ parameter characterizing the oscillator non-isochronity (see Figure 9,b). With the further growth of r_n, the asymptotic damping of "oscillations" in dynamic phase variations $\Delta\delta_{DD}$ is also observed.

Results obtained here seem to be contradictory to usual insides [12] and have the entirely explainable physical sense. To understand it, it is enough to turn to the simplified model of interaction process of the autodyne oscillator with the proper reflected emission, which was considered in [22] by means of a stepping method using an example of radio-pulse, autodyne. From this model, it follows that with shortening of the relative pulse duration (which is equivalent to growth of normalized distance), a number of partial reflections decreases during radio pulse action. This leads to reduction of the equivalent feedback parameter C_{eq} of autodyne system and, accordingly, to decrease of the signal distortion level. At achievement of the normalized distance equaled to $(r_n = 1)$, when the reflected emission impact becomes one-partial, the formation of practically sine autodyne variations of amplitude and frequency are provided.

6 Results of Experimantal Investigations

Experimental investigations of FM ASRR signal peculiarities were preformed with oscillating module on the 8mm-range Gunn diode in the autodyne sensor structure developed for monitoring of the point crossing occupation on the hump yard [4–6].

Figure 10 shows the total view of the sensor and its main components. An antenna with an UHF module and the printed board for probing signal formation, digital signal processing and coupling interface RS-485 are placed into cylindrical encapsulated case from duralumin by 92mm-diameter and 170mm-length. The dielectric lens of the antenna is simultaneously the forward wall of the case.

a) b) c)

Figure 10: Total view of the autodyne sensor (a) of the autodyne module with a horn antenna (b) and the printed board (c) of the unit for control and signal processing

The autodyne UHF module of the sensor is performed on the base of the Gunn diode AA727A and the varicap 3A637A-6 in the packaged fabrication. The output power is 25 mW, the central frequency is 36.5 GHz. The UHF module provides in the linear FM mode the frequency deviation in the 500 MHz band. The FM law is symmetric or non-symmetric saw-tooth with modulation frequency of 10 kHz.

The autodyne signal is extracted in the power source circuit of the Gunn diode with the help of the wideband current transformer. After filtering and amplification, it passes to ADC of the digital signal processor (DSP) TMS320F2808 from Texas Instruments in the processing unit. In this unit, functions of modulating voltage formation, digital signal processing and the communication interface RS-485 with PC are realized with software.

The computing kernel of DSP performs the digital signal processing (filtering and the Fourier analysis), which results are transferred through the universal asynchronous transceiver to PC used as a mapping system of radar information. When the reflecting object is situated in the ASRR antenna pattern, then at output of the one of spectrum analyzer's filters of DSP the signal will be present. Its amplitude characterizes the reflecting capability of the object under investigation, while a filter number, in which the useful signal arrives, characterizes the distance from ASRR to the object.

To exclude from the received signal spectrum of components associated with PAM and reflections from the near objects the information not interesting for us, before the Fourier transform in DSP we use signal pre-filtering. For this, the algorithm of "moving average" is used to the initial signal, and this algorithm serves as the low-pass filter. After extraction of low-frequency components by this filter, they are subtracted from the initial signal, and as a result, the "dead zone" is formed near ASRR of one-meter-order distance. The high-frequency signal components remaining at the filter output contain information about reflecting objects being in the required distance range.

Figure 11 shows signal spectrograms obtained from the arriving (a), fixed (b) and departing (c) reflecting object if we use in ASRR non-symmetric saw-tooth FM law. For mentioned cases Figure 12 presents the spectrograms for symmetric FM law. The electrical-mechanical imitator of the Doppler signal [23] was used as the reflecting object.

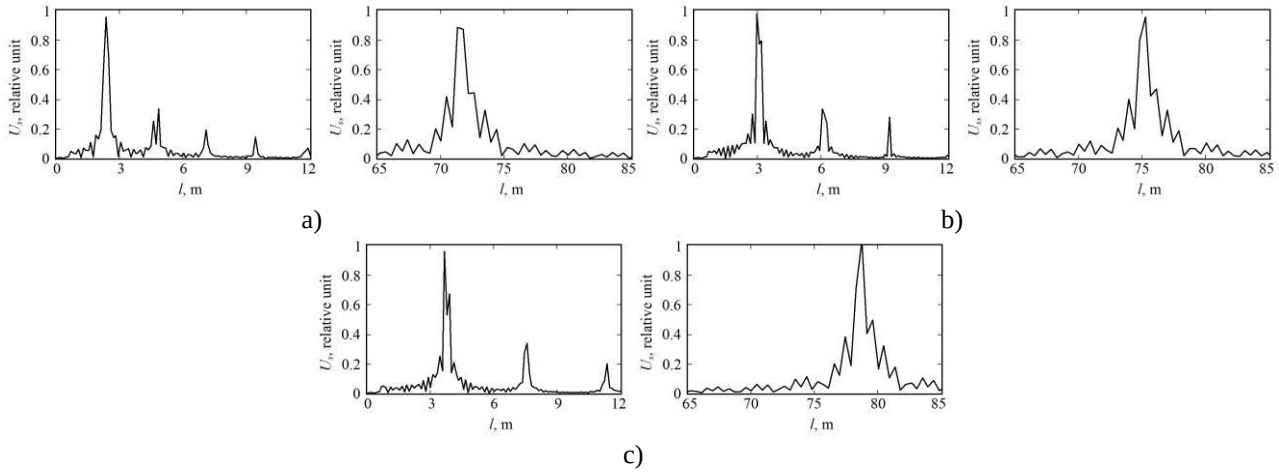

Figure 11: Spectrograms of signals transformed by the autodyne obtained from the arriving (a), fixed (b) and departing (c) reflecting object (an imitator) at the non-symmetric saw-tooth FM

In the first group of experiments, the distance from ASRR to the imitator was 3 m (see left spectrograms in Figures 11 and 12), while in the second group – 75 м (see right spectrograms in Figures 11 and 12). In the first experiments, we attach the horn antennas to the UHF module and the imitator with the pattern width $10^0 \times 10^0$ degrees for the -3dB-level and with gain about 25 dB. In the second group we used double-mirror antennas with the elliptical small mirror with the pattern width 1.4×1.4 degrees and with gain about 42 dB. Signal amplitude (Us) in both experiments were aligned with the help of the variable attenuator inserting between the UHF module and the antenna. At that, the attenuator damping was set in such a manner to provide $C_{FB} \approx 0.8$.

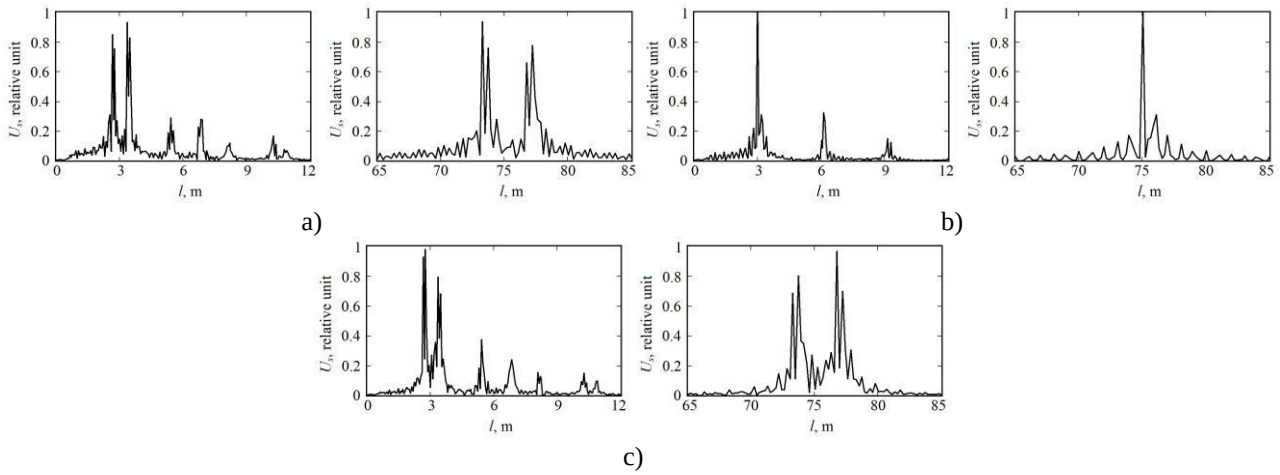

Figure 12: Spectrograms of signals transformed by the autodyne obtained from arriving (a), fixed (b) and departing (c) reflected object (an imitator) for symmetric saw-tooth FM law.

Motion direction of the reflecting object was changed by switching of the rotation direction of electric motor, which shaft is connected to the reflector in the Doppler signal imitator [23]. In the case of a fixed object, the power was switched-off from the motor and reflector was stopped.

The first experiment on the ratio of the delay time τ of the reflected signal and the T_a period in both cases of used modulation laws corresponds to the beginning of the first operation zone $\mathrm{r_n} \ll 1$. In the second experiment for the non-symmetric FM law, the normalized distance is $\mathrm{r_n} = 1.25$, and $\mathrm{r_n} = 2.5$ for the symmetric law.

At utilization of the saw-tooth non-symmetric FM law, the moving reflector causes the spectrum shift towards frequency decrease when object arriving while frequency increase when departing from ASRR (see Figure 11). At utilization of the saw-tooth symmetric FM law, the moving reflector causes spectrum "splitting" into two "side" components, which are shifted from the average frequency value by Doppler shift (see Figure 12). These statements are agreed with the general theory of FM ASRR operation [9].

In the first experiment (see left diagrams in Figures 11, 12) the noticeable level of the second and third higher harmonics are seen, which is typical for anharmonic distortions of the autodyne signal. In the second experiment (see right diagrams) higher harmonic level is essentially lower than in the previous case. These results are new; they confirm the above-mentioned conclusions of the theoretical examination.

Thus, experimental data obtained confirm the adequacy of the above-developed mathematical model for analysis and calculations of signal and spectral characteristics of FM ASRRs.

7 Conclusions

Accordingly, the peculiarities of ASRR signal formation for linear FM obtained from the moving reflecting object are considered in this paper. The general case of arbitrary ratio of delay time □ of the reflected emission and the signal T_a period is described.

Fulfilled calculations and experimental investigations of FM ASRR show that the autodyne signal frequency both for moving and fixed reflector correspond exactly to the transformed signal frequency which is obtained in the case of the homodyne system [9, 12]. Nevertheless, the presence of autodyne signal distortions and spectrum enrichment under conditions when the distance to the reflected object is small and when $C_{FB} > 0$, the inequality $\tau \ll T_a$ is satisfied and require to take these into consideration in the devices of their processing.

Research results obtained of the autodyne characteristics for the case, when the autodyne response period is commensurable or even smaller than the delay time of the reflected emission, show that the distortion level of the autodyne signals decreases with the reflected object distance growth at hypothetical keeping of the reflected wave amplitude. From this, it follows that under condition when the feedback parameter value, which sometimes exceeds of its

boundary value, in higher operation zones of FM ASRR, the stable oscillator operation with formation of quasi-harmonic signals can be ensured.

Analysis results obtained in this paper develop and expand the known research results performed in [22, 24], in account of oscillator FM as well as the results fulfilled in [10–12] in account of dynamics of reflected emission phase variation in the autodyne model at wave propagation to the object and back. Regulations revealed of signal formation in FM ASRR have the sufficiently general character and clear physical interpretation on the base of the stepping method known from the theory of retarded systems. In this connection, the results obtained, as we think, can be also used at calculation of autodyne system signals, which are made on the base of semiconductor laser modules [13–15].
Additional confirmation of developed model adequacy of FM ASRR signals is the successful functioning of some systems created on the base of 8mm-range Gunn diodes [4–6].

Acknowledgment

The present paper is prepared in accordance with an Agreement on scientific-technological cooperation between UrFU and IRE NASU, as well as at financial support of Russian Federation Government, order № 211, contract № 02. A03.21.0006.

References

1. B.M. Armstrong, R. Brown, F. Rix and J.A.C. Stewart, “Use of Microstrip Impedance-Measurement Technique in the Design of a BARITT Diplex Doppler Sensor,” IEEE Transactions on Microwave Theory and Techniques, 1980, vol. MTT-28, no. 12, pp. 1437-1442. doi: 10.1109/TMTT.1980.1130263
2. A. Efanov, K. Lübke, Ch. Diskus, A. Springer, A. Stelzer and H.W. Thim, “Development of a 35 GHz Radar Sensor,” Proceedings of the seminar “Basics and Technology of Electronic Devices.” Pongau, Austria, 1997, pp. 11-16.
3. S.A. Alidoost, R. Sadeghzade and R. Fatemi, “Autodyne System with a Single Antenna,” 11th International Radar Symposium (IRS-2010). Vilnius, Lithuania, 2010, vol. 2, pp. 406-409.
4. A.V. Varavin, A.S. Vasiliev, G.P. Ermak and I.V. Popov, “Autodyne Gunn-diode transceiver with internal signal detection for short-range linear FM radar sensor,” Telecommunication and Radio Engineering, 2010, vol. 69, no. 5, pp. 451-458. doi: 10.1615/TelecomRadEng.v69.i5.80
5. G.P. Ermak, I.V. Popov, A.S. Vasilev, A.V. Varavin, V.Ya. Noskov and K.A. Ignatkov, “Radar sensors for hump yard and rail crossing applications,” Telecommunication and Radio Engineering, 2012, vol. 71, no. 6, pp. 567-580. doi: 10.1615/TelecomRadEng.v71.i6.80
6. V.Ya. Noskov, A.V. Varavin, A.S. Vasiliev, G.P. Ermak, N.M. Zakarlyuk, K.A. Ignatkov and S.M. Smolskiy, “Sovremennyie gibridno-integralnyie avtodinnyie generatoryi mikrovolnovogo i millimetrovogo diapazonov i ih primenenie. Ch. 9. Radiolokatsionnoe primenenie avtodinov,” [Modern hybrid-integrated autodyne oscillators of microwave and millimeter wave ranges and their application. Part 9. Autodyne radar applications], Uspehi sovremennoy radioelektroniki [Successes of modern electronic engineering], 2016, no. 3, pp. 32-86. (in Russian).
7. P.A. Jefford and M.S. Howes, “Modulation schemes in low-cost microwave field sensor,” IEEE Transaction of Microwave Theory and Technique, 1985, vol. MTT-31, no. 8, pp. 613-624. doi: 1109/TMTT.1983.1131559
8. S.D. Votoropin and V.Ya. Noskov, “Analysis of operating regimes of EHF hybrid-integrated autodynes based on the Gunn micro power mesa planar diodes,” Russian Physics Journal, 2002, vol. 45, no. 2, pp. 195-206 doi: 10.1023/A:1019664300993.
9. I.V. Komarov and S.M. Smolskiy, “Fundamentals of short-range FM radar.” Norwood: Artech House, 2003. 289p. doi: 1109/MAES.2004.1346903
10. S.D. Votoropin, V.Ya. Noskov and S.M. Smolskiy, “An analysis of the autodyne effect of oscillators with linear frequency modulation,” Russian Physics Journal, 2008, vol. 51, no. 6, pp. 610-618. doi: 1007/s11182-008-9083-5
11. S.D. Votoropin, V.Ya. Noskov and S.M. Smolskiy, “An analysis of the autodyne effect of a radio-pulse oscillator with frequency modulation,” Russian Physics Journal, 2008, vol. 51, no. 7, pp. 750-759. doi: 1007/s11182-008-9105-3.

12. S.D. Votoropin, V.Ya. Noskov and S.M. Smolskiy, “Sovremennyie gibridno-integralnyie avtodinnyie generatoryi mikrovolnovogoi millimetrovogo diapazonov i ih primenenie. Chast 5. Issledovaniya avtodinov s chastotnoi modulyaciei,” [Modern hybrid-integrated autodyne oscillators of microwave and millimeter ranges and their application. Part 5. Investigations of frequency-modulated autodynes], Uspehi sovremennoy radioelektroniki [Successes of modern electronic engineering], 2009, no. 3, pp. 3-50. (in Russian).
13. G. Giuliani, M. Norgia, S. Donati and T. Bosch, “Laser diode self-mixing technique for sensing applications (Review article),” Journal of Optics A: Pure and Applied Optics, 2002, vol. 4, no. 6, pp. 283-294.
14. V.S. Sobolev and G.A. Kashcheeva, “Self-mixing frequency-modulated laser interferometry,” Optoelectronics, Instrumentation and Data Processing, 2008, vol. 44, no. 6, pp. 519-529. doi: 10.3103/S8756699008060058
15. D.A. Usanov, A.V. Skripal and E.I. Astakhov, “Determination of nanovibration amplitudes using frequency-modulated semiconductor laser autodyne,” Quantum Electronics, 2014, vol. 44, no. 2, pp. 184-188. doi : 10.1070/QE2014v044n02ABEH015176
16. V.Ya. Noskov, A.S. Vasiliev, G.P. Ermak, K.A. Ignatkov and A.P. Chupahin, “Mathematical model of FM autodyne radar,” Proc. The 9-th International Kharkov Symposium on Physics and Engineering of Microwaves, Millimeter and Submillimeter Waves (MSMW'16). Kharkov, Ukraine, 2016, A-25, pp. 1-4. doi: 10.1109/MSMW.2016.7538000
17. K.A. Ignatkov and A.S. Vasiliev, “Signals of the autodyne FM radar for mm-wavelength range,” 26-th International Crimean Conference “Microwave & Telecommunication Technology” (CriMiCo’2016). Sevastopol, Russia, 2016, vol. 10, pp. 2139-2145.
18. V.Ya. Noskov and K.A. Ignatkov, “Autodyne signals in case of random delay time of the reflected radiation,” Telecommunication and Radio Engineering, 2013, vol. 72, no. 16, pp. 1521-1536. doi: 10.1615/TelecomRadEng.v72.i16.70
19. V.Ya. Noskov and G.P. Ermak, “Signal and fluctuation characteristics of autodyne vibration and displacement meters,” Telecommunication and Radio Engineering, 2014, vol. 73, no. 19, pp. 1727-1743. doi: 10.1615/TelecomRadEng.v73.i19.30
20. V.Ya. Noskov and K.A. Ignatkov, “About applicability of quasi-static method of autodyne systems analysis,” Radioelectronics and Communications Systems, 2014, vol. 57, no. 3, pp. 139-148. doi: 10.3103/S0735272714030054.
21. B.P. Lathi, “Communication systems,” John Wiley & Sons, Inc, New York, 1968. 320 p.
22. V.Ya. Noskov and K.A. Ignatkov, “Dynamics of autodyne response formation in microwave generators,” Radioelectronics and Communications Systems, 2013, vol. 56, no. 5, pp. 227-242. doi: 10.3103/S0735272713050026
23. V.Ya. Noskov, K.A. Ignatkov and S.M. Smolskiy, “Zavisimost avtodinnih harakteristik ot vnutrennih parametrov SVCh generatorov,” [Autodyne Characteristic Dependence on the UHF Oscillator’s Inherent Parameters], Radiotecnika, 2012, no. 6, pp. 24-42. (in Russian).
24. V.Ya. Noskov and K.A. Ignatkov, “Dynamic features of autodyne signals,” Russian Physics Journal, 2013, vol. 56, no. 4, pp. 420-428. doi: 10.1007/s11182-013-0051-3